BIOCHEMISTRY
including biophysical chemistry & molecular biology

Article

pubs.acs.org/biochemistry

Identification of Interactions Involved in the Generation of Nucleophilic Reactivity and of Catalytic Competence in the Catalytic Site Cys/His Ion Pair of Papain

Syeed Hussain,[†] Akavish Khan,[†] Sheraz Gul,[†,⊥] Marina Resmini,[‡] Chandra S. Verma,[§] Emrys W. Thomas,[∥] and Keith Brocklehurst*[,†]

[†]Laboratory of Structural and Mechanistic Enzymology, School of Biological and Chemical Sciences, Fogg Building, Queen Mary, University of London, Mile End Road, London E1 4NS, U.K.

[‡]School of Biological and Chemical Sciences, Joseph Priestly Building, Queen Mary, University of London, Mile End Road, London E1 4NS, U.K.

[§]Bioinformatics Institute, 30, Biopolis Way, #07-01 Matrix, Singapore 138671

[∥]Department of Biological Sciences, University of Salford, The Crescent, Salford M5 4JW, U.K.

ABSTRACT: Understanding the roles of noncovalent interactions within the enzyme molecule and between enzyme and substrate or inhibitor is an essential goal of the investigation of active center chemistry and catalytic mechanism. Studies on members of the papain family of cysteine proteinases, particularly papain (EC 3.4.22.2) itself, continue to contribute to this goal. The historic role of the catalytic site Cys/His ion pair now needs to be understood within the context of multiple dynamic phenomena. Movement of Trp177 may be necessary to expose His159 to solvent with consequent decrease in its degree of electrostatic solvation of (Cys25)-S^-. Here we report an investigation of this possibility using computer modeling of quasi-transition states and pH-dependent kinetics using 3,3′-dipyridazinyl disulfide, its *n*-propyl and phenyl derivatives, and 4,4′-dipyrimidyl disulfide as reactivity probes that differ in the location of potential hydrogen-bonding acceptor atoms. Those interactions that influence ion pair geometry and thereby catalytic competence, including by transmission of the modulatory effect of a remote ionization with pK_a 4, were identified. A key result is the correlation between the kinetic influence of the modulatory trigger of pK_a 4 and disruption of the hydrogen bond donated by the indole N−H of Trp177, the hydrophobic shield of the initial "intimate" ion pair. This hydrogen bond is accepted by the amide O of Gln19—a component of the oxyanion hole that binds the tetrahedral species formed from the substrate during the catalytic act. The disruption would be expected to contribute to the mobility of Trp177 and possibly to the effectiveness of the binding of the developing oxyanion.

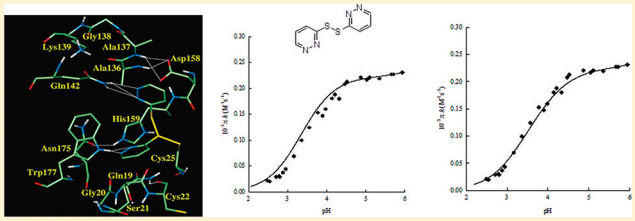

In enzyme function noncovalent interactions (reviewed in ref 1) are not restricted to specific recognition of substrates but are involved in catalysis in a variety of ways that contribute to transition state stabilization. Mechanistically important effects of such interactions within the enzyme molecule and between enzyme and substrate or time-dependent inhibitor continue to be exemplified and illuminated by studies on the papain family of cysteine proteinases (e.g., refs 2−9). Many aspects of the cysteine proteinase (cysteine peptidase) superfamily, which comprises six enzyme families[10] widely distributed in nature, are reviewed in ref 11. More recent reviews[12,13] deal with the active center chemistry and catalytic mechanism of the papain family (see e.g. refs 6, 14, and 15). This family contains the best-characterized and most intensively studied member of the superfamily, papain itself (EC 3.4.22.2.).

The minimal model of catalysis of the hydrolysis of an amide or ester substrate by a cysteine proteinase involves formation of an acylenzyme (thiolester) intermediate (ES′) together with the amine or alcohol product (P_1) by reaction via a tetrahedral species within an adsorptive complex (ES), followed by hydrolysis (deacylation) of ES′ which provides the carboxylate product (P_2) (see refs 12 and 13 for a discussion of the evidence for these events). For many years a generally assumed concept of central importance in the catalytic mechanism of these enzymes was that catalytic competence develops synchronously with and consequent upon formation of the (Cys25)-S^-/(His159)-Im^+H ion pair state (papain numbering) by proton loss from (Cys25)-SH associated with pK_a 4, the common value across which catalytic competence develops with increase in pH as reflected by k_{cat}/K_m. This concept was shown to be incorrect, however, by a combination of reactivity probe kinetics using 2-pyridyl and 4-pyrimidyl disulfides, kinetics of catalysis, and electrostatic potential calculations for papain and some natural variants, e.g., caricain [papaya proteinase Ω, EC 3.4.22.3].[6] Thus, the ion pair state is now known to be produced by protonic dissociation from (Cys25)-

Received: August 3, 2011
Revised: October 24, 2011
Published: November 1, 2011

SH/(His159)-Im$^+$H across pK_a 3.35 in papain and 2.90 in caricain, i.e., lower than 4, and is not catalytically competent. Rather, protonic dissociation from an electrostatic modulator (pK_a 4) in both papain and caricain, possibly a component of the electrostatic clusters associated with Glu50, is required for catalysis. These clusters are similar in both enzymes, the only difference being that residue 17 is Lys in papain and Arg in caricain. The Glu50 cluster, which is remote from Asp158, is one of the nearest carboxylate clusters to the Cys25/His ion pair and includes the three carboxylates (those of Glu35, Glu52, and Glu50 itself) that contribute the highest interaction energies with it in both enzymes.[6] The modulator cannot be the Asp158 carboxy group despite the fact that it is the individual ionizable group nearest the catalytic site ion pair, whose possible role in active center chemistry has been much discussed,[12,13] because its pK_a value is now known to be 2.8 in papain and 2.0 in caricain.[15,16] (Asp158)-CO_2^- may be an additional electrostatic influence[5,17] but, if so, is permanently in the "on" state in the pH range over which catalytic activity develops.

A key objective related to but not identical with the development of catalytic competence in these enzymes is to understand the phenomena responsible for the generation of nucleophilic reactivity in the catalytic site Cys/His ion pair, which may be regarded as a necessary event in the pH-dependent chemistry of the catalytic mechanism. A working hypothesis is that this might involve decrease in the effectiveness of the mutual solvation of the anionic (S^-) and cationic (Im$^+$H) partners of an "intimate" ion pair of low or zero nucleophilic reactivity present at low pH.[9] This is envisaged to be followed by further perturbation of ion pair geometry to allow the partners to play their respective roles of nucleophile and general acid catalyst in the rate-determining acylation process of the catalytic act as the pH increases across pK_a 4, a consequence of the ionization of the electrostatic modulator[6] coupled with specific P_2−S_2 and transcleft binding interactions.[3] Because the modulator with pK_a 4 appears to be remote from the immediate catalytic site, any hypothesis for its mechanism of modulation of ion pair geometry must necessarily include the transmission interactions, some of which might be close to the catalytic site. We recently reported evidence using papain[9] for one aspect of the overall hypothesis (generation of nucleophilic reactivity and of catalytic competence and transmission initiated by protonic dissociation with pK_a 4) using cationic aminoalkyl 2-pyridyl disulfide reactivity probes (**1**−**3**, Figure 1). These probes were designed to bind with various degrees of effectiveness near both Asp158 and Trp177 of papain as well as to react with Cys25. Enzyme−probe interactions that determine the presence or absence of nucleophilic reactivity in Cys25 at low pH were identified by comparing the pH−second-order rate constant (k) profiles for the reactions of papain with probes **1**−**4**, together with computer modeling. The existence of nucleophilic reactivity at low pH is readily demonstrated using simple alkyl-2-pyridyl disulfide probes such as *n*-propyl-2-pyridyl disulfide (**4**) by the presence of a bell-shaped component with high reactivity. Protonation of the pyridyl ring provides the probe with enhanced reactivity which makes it a sensitive detector of nucleophilicity, particularly derived from low pK_a thiol groups.[18] A striking low-pH bell is present in the pH−k profiles for the reactions with the simple alkyl probe **4** and with the longest aminoalkyl probe **3** containing a four-methylene spacer. This contrasts markedly with the absence of high-

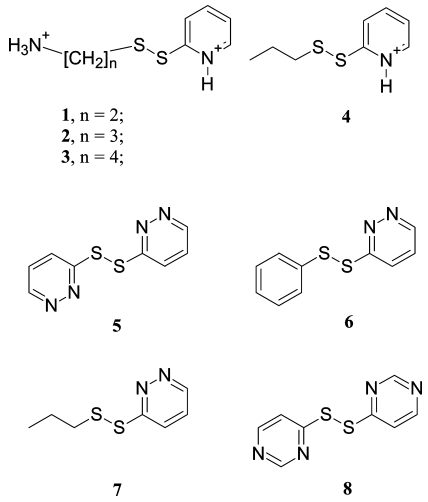

Figure 1. The 2-pyridyl disulfide reactivity probes **1**−**4**, shown in fully protonated cationic forms, used in a previous study[9] and the 3-pyridazinyl probes **5**−**7** and 4,4′-dipyrimidyl disulfide (**8**) used in the present work shown in nonprotonated neutral forms; pK_a values of their monoprotonated forms for **5**, 0.51; for **6**, 0.92; for **7**, 1.23; and for **8**, 0.91.

reactivity bells for the reactions with the shorter aminoalkyl probes **1** and **2** containing only two or three methylene spacers, respectively. This difference prompted the investigation by modeling of the binding modes of the two sets of probes, i.e., those associated with the lack (**1** and **2**) and the presence (**3** and **4**) of substantial nucleophilic reactivity in Cys25 at low pH. In the quasi-transition states of the reactions of papain with probes **3** and **4** the protonated pyridyl ring is bound remotely from Trp177. By contrast, in the reactions with probes **1** and **2** the protonated pyridyl ring is bound in the proximity of the indole ring system of Trp177. These results, together with associated normal-mode analysis, suggest the possibility that release of nucleophilic reactivity in Cys25 requires decrease in the solvation of (Cys25)-S^- by (His159)-Im$^+$H occasioned by movement of the cleft around Trp177, which is restricted by the protonated pyridyl rings of **1** and **2**.[9]

The evidence for the hypothesis described in ref 9, involving movement of the cleft around Trp177, derives from the use of the dicationic probes **1** and **2** containing both protonated amino substituents that engage Asp158 and protonated pyridyl rings. It was essential, therefore, to design electrically neutral probes to eliminate direct electrostatic interactions between enzyme and probe. Instead, combinations of hydrogen-bonding sites would be provided with the potential of both influencing the movement of Trp177 and engaging other sites proximal to the immediate catalytic site to begin to identify those nonelectrostatic interactions that influence ion pair geometry, including by transmission of the effect of the remote ionization with pK_a 4 and thus nucleophilic reactivity and catalytic competence. In the present paper we describe the choice for this investigation, influenced by preliminary modeling, of three pyridazinyl probes (**5**−**7**) and their synthesis, characterization, and use in mechanism-targeted kinetic studies, together with 4,4′-dipyrimidyl disulfide (**8**) in which N-3 of the pyridazinyl ring is replaced by N-4 of the pyrimidyl ring. The symmetrical pyridazinyl probe **5** differs from the symmetrical pyrimidyl probe **8** in the position of one of the ring N atoms which provides variation in hydrogen-bonding possibilities. The phenyl pyridazinyl probe **6** is similar in steric occupancy to **5**

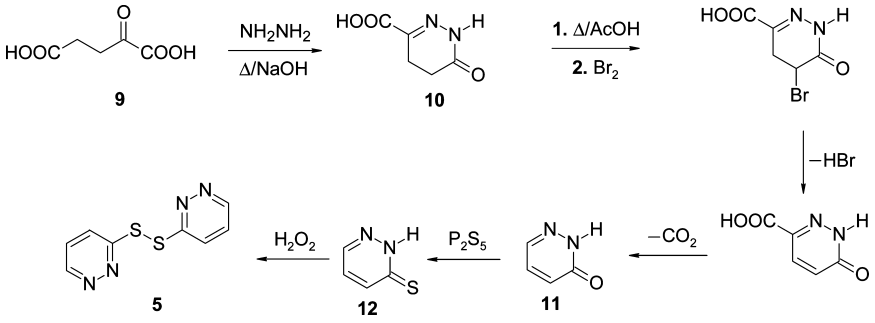

Figure 2. Synthetic route to the symmetrical chromogenic reactivity probe 3,3′-dipyridazinyl disulfide (**5**). Reaction of **5** with a thiol-containing molecule results in the release of the chromophoric pyridazine-3-thione (**12**).

but differs in that the nonleaving (phenyl) group is devoid of hydrogen-bonding sites. By contrast, the *n*-propylpyridazinyl probe **7** contains a smaller and more flexible nonleaving group predicted to additionally perturb the binding mode.

EXPERIMENTAL PROCEDURES

Enzymes: Purification and Active Site Titration. Initial stages in the purification of papain[19] and caricain[14] involved salt fractionation and anion exchange chromatography. Production of fully active enzymes containing 1 mol of functional catalytic site per mole of enzyme was by proton-activated covalent chromatography,[20,21] reviewed in ref 22. Active site titration was by spectrophotometric titration at 343 nm [$\Delta\varepsilon_{343} = 8.08 \times 10^3/(1 + K_a/[H^+])$ M^{-1} cm^{-1}, where $pK_a = 9.8$[23]], using 2,2′-dipyridyl disulfide as a two-protonic-state titrant[18] at pH 4 and pH 8.[24] Identical instantaneous values of $\Delta\varepsilon_{343}$, indicating the yield of the thiolysis product, pyridine-2-thione, at each of these pH values establishes the absence of both contaminant low-M_r mercaptans and nonenzymatically active but thiol-containing protein including denatured cysteine proteinase.

Synthesis of the Symmetrical Reactivity Probe 3,3′-Dipyridazinyl Disulfide (5, Figure 1). The six-step synthesis is shown in Figure 2. The first four steps were carried out as described in ref 25: reaction of 2-ketoglutaric acid (**9**) with hydrazine sulfate in the presence of base via a hydrazone intermediate (not shown) produced 1,4,5,6-tetrahydro-6-oxopyridazine-3-carboxylic acid (**10**). In the next three steps, acid-catalyzed enol formation and bromination, elimination of HBr, and decarboxylation provided the intermediate 3-pyridazone (**11**). Synthesis of **5** from **11** involved thionation by P_2S_5 to provide pyridazine-3-thione (**12**) followed by H_2O_2 oxidation to the disulfide **5** as described below.

3-Pyridazone (10 g) in dry piperidine (100 mL) containing P_2S_5 (10 g) was heated under reflux with efficient stirring for 80 min and then cooled by addition of H_2O (50 mL) and evaporated to dryness *in vacuo* at <50 °C. The resulting tar was extracted several times with boiling EtAc (500 mL portions) to extract the bright yellow pyridazine-3-thione (**12**), which was obtained in crude form by evaporation to dryness *in vacuo*. This was suspended with rapid stirring in H_2O (15 mL), and H_2O_2 (1.5 mL of 27.5% solution) was added dropwise over 15 min at room temperature (~22 °C). Stirring was continued at room temperature for a further 2 h, during which time the yellow color of the thione disappeared as a consequence of formation of the disulfide **5**. This was isolated by filtration, air-dried, and crystallized from boiling EtAc during slow cooling to produce large crystalline plates of pure **5**, mp 132−135 °C. Thiolysis of a sample of the final product at pH 6.0 by 2-mercaptoethanol produced the predicted yield of pyridinzine-3-thione (**12**) deduced by spectral analysis at 355 nm (where the absorption of **5** is negligible), quantified by using $\Delta\varepsilon_{355} = 2.83 \times 10^3$ M^{-1} cm^{-1}. MS (EI): m/z 222 [$M^+ + 1$] 223, $C_8H_6N_4S_2$ requires [M^+] 222. ^{1}H NMR (400 MHz, $CDCl_3$): δ 7.46 (dd, J = 8.7, 5.0 Hz, 2H), 7.89 (d, J = 8.7 Hz, 2H), 9.05 (d, J = 5.0 Hz, 2H). ^{13}C NMR ($CDCl_3$): δ 124.4, 127.4, 149.7 163.1.

Synthesis of Phenyl-3-pyridazinyl Disulfide (6, Figure 1). To a solution of 3,3′-dipyridazinyl disulfide, **5** (1.1 g, 5 mmol), in CH_3OH/CH_2Cl_2 (1:1, v/v), Et_3N (0.42 mL, 3 mmol) was added, and the resulting solution was stirred rapidly during the dropwise addition of thiophenol (0.33 g, 3 mmol) over 30 min. Stirring was continued for a further 2 h at room temperature, after which the solvent was removed *in vacuo*, and following the addition of 5% citric acid (50 mL) the mixture was kept at 4 °C for 12 h. The required product **6** was contained in an oily precipitate that was washed with water by decantation. It was then dissolved in CH_2Cl_2, and **6** was freed from residual **5** and diphenyl disulfide by column chromatography (Al_2O_3; eluant, CH_2Cl_2) and crystallized from petroleum ether (bp 160−170 °C) as white needles, mp 88 °C. Thiolysis of a sample as described for **5** produced the expected yield of **12**. MS (EI): m/z 221 [$M^+ + 1$] 223, $C_{10}H_8N_2S_2$ requires [M^+] 220. ^{1}H NMR (400 MHz, $CDCl_3$): δ 7.26 (d, J = 4.5 Hz 1H), 7.32 (dd, J = 7.8, 4.5 Hz, 2H), 7.41 (dd, J = 8.8, 4.4 Hz, 1H), 7.52 (d, J = 7.8 Hz, 2H), 7.85 (d, J = 8.8 Hz, 1H), 9.01 (d, J = 4.4 Hz, 1H). ^{13}C NMR ($CDCl_3$): δ 123.6, 127.2, 127.6, 127.8, 129.4, 135.0, 149.1, 164.8.

Synthesis of *n*-Propyl-3-pyridazinyl Disulfide (7, Figure 1). This procedure is analogous to that described for **6** using *n*-propanethiol (0.38 g, 5 mmol) instead of thiophenol; **7**, purified by column chromatography is a pale green oil. Thiolysis of a sample as described for **5** produced the expected yield of **12**. MS (EI): m/z 187 [$M^+ + 1$] 187, $C_7H_{10}N_2S_2$ requires [M^+] 186. ^{1}H NMR (400 MHz, $CDCl_3$): δ 1.0 (t, J = 8 Hz, 3H), 1.73 (m, 2H), 2.8 (t, J = 8 Hz, 2H), 7.45 (dd, J = 9, 4.5 Hz, 1H), 7.95 (d, J = 9 Hz, 1H), 9.0 (d, J = 4.5 Hz, 1H). ^{13}C NMR ($CDCl_3$): δ 13.04, 22.28, 41.02, 123.56, 126.86, 148.86, 165.50.

Determination of the Spectroscopic Characteristics and of the pK_a Values of the 3-Pyridazinyl Disulfide Reactivity Probes (5− 7) and the Thiolysis Product Pyridazine-3-thione (12). Electronic absorption spectra (230−500 nm) of solutions in aqueous buffers of **5**−**7** and **12** were recorded at constant concentration in the pH range −0.3−12 at 25 °C. The pK_a values of the monoprotonated forms of **5**−**7** were determined from the decrease in the extinction coefficient (ε) of the shoulder at 315 nm with

increase in pH and that of the neutral molecule **12** from the decrease in ε of the long wavelength band at λ_{max} 355 nm with increase in pH, as detailed below.

The value of the observed extinction coefficient (ε) of a mixture of a weak acid (dissociation constant K_a) and its conjugate base, both of which absorb at a common wavelength but with different values of their respective pH-independent extinction coefficients $\tilde{\varepsilon}_1$ and $\tilde{\varepsilon}_2$, is provided by the sum of the two terms of eq 1. This equation can be written with a denominator that is common to both terms as eq 2.

$$\varepsilon = \frac{\tilde{\varepsilon}_1}{1 + \frac{K_a}{[H^+]}} + \frac{\tilde{\varepsilon}_2}{1 + \frac{[H^+]}{K_a}} \quad (1)$$

$$\varepsilon = \frac{\tilde{\varepsilon}_1[H^+] + \tilde{\varepsilon}_2[K_a]}{[K_a] + [H^+]} \quad (2)$$

A plot of ε vs pH is of quasi-sigmoid form in which ε approaches the pH-independent values $\tilde{\varepsilon}_1$ and $\tilde{\varepsilon}_2$ at low and high pH, respectively. For example, at high pH when $[H^+] \ll K_a$, ε approaches closely to $\tilde{\varepsilon}_1[H^+]/K_a + \tilde{\varepsilon}_2$, and when ε becomes pH-independent, the value of $\tilde{\varepsilon}_1[H^+]/K_a$ has become negligible so that $\varepsilon = \tilde{\varepsilon}_2$. Subtraction of $\tilde{\varepsilon}_2$ from both sides of eq 2 gives eq 3, which simplifies to eq 5 via eq 4, and the reciprocal form of eq 5 is eq 6.

$$\varepsilon - \tilde{\varepsilon}_2 = \varepsilon' = \frac{\tilde{\varepsilon}_1[H^+] + \tilde{\varepsilon}_2 K_a}{K_a + [H^+]} - \tilde{\varepsilon}_2 \quad (3)$$

$$\varepsilon' = \frac{\tilde{\varepsilon}_1[H^+] + \tilde{\varepsilon}_2 K_a - \tilde{\varepsilon}_2 K_a - \tilde{\varepsilon}_2[H^+]}{K_a + [H^+]} \quad (4)$$

$$\varepsilon' = \frac{\tilde{\varepsilon}_1 - \tilde{\varepsilon}_2}{1 + \frac{K_a}{[H^+]}} \quad (5)$$

$$\frac{1}{\varepsilon'} = \frac{1}{\tilde{\varepsilon}_1 - \tilde{\varepsilon}_2} + \frac{K_a}{\tilde{\varepsilon}_1 - \tilde{\varepsilon}_2}\frac{1}{[H^+]} \quad (6)$$

The ε_{315}–pH data for **5**–**7** and the ε_{335}–pH data for **12** were analyzed by linear regression of $1/\varepsilon'$ on $1/[H^+]$ using eq 6 to provide best fit values of K_a.

In principle, providing that both $\tilde{\varepsilon}_1$ and $\tilde{\varepsilon}_2$ can be accurately determined by inspection of extensive pH-independent values of ε in the low and high pH plateaus, the pK_a can be calculated using eq 2 as the pH value corresponding to $\varepsilon = (\tilde{\varepsilon}_1 - \tilde{\varepsilon}_2)/2$.

Stopped-Flow (SF) Kinetics. Kinetic studies on the reactions of the catalytic site thiol group of papain with the reactivity probes were performed by using an Applied Photophysics SFMV stopped-flow spectrophotometer, kinetics workstation, and data acquisition and analysis software. Monochromator entrance and exit slits widths were set at 0.5 mm. Temperature control was by a Grant LTD6 water bath by thermostatically controlled temperature cycling. Complete absorbance (A) versus time (t) progress curves for the reactions of the enzymes with the reactivity probes (R) were recorded by monitoring the release of the chromophoric product pyridazine-3-thione[11] at 355 nm ($\Delta\varepsilon_{355} = 2.83 \times 10^3$ M^{-1} cm^{-1}). All reactions were carried out under pseudo-first-order conditions with $[R]_0 \gg$ [enzyme] at 25 °C in aqueous buffer at I = 0.1 M and containing 1 mM EDTA. Pseudo-first-order rate constants (k_{obs}) were computed by fitting the A–t data to an equation for a single-exponential process, i.e., $A = P_1e^{-P_2t} + P_3$, where $P_1 = A_\infty - A_0$, $P_2 = k_{obs}$, and $P_3 = A_\infty$. In all cases an average of at least three essentially superimposable traces was used to provide k_{obs} (SD < 10%). Linear dependence of k_{obs} (s^{-1}) on $[R]_0$ demonstrated overall second-order kinetics and the second-order rate constants (k) were obtained by dividing k_{obs} by $[R]_0$.

Computer evaluation of pH-dependent kinetic data was carried out by a combination of curve sketching using the multitasking application program, SKETCHER, and weighted nonlinear regression using Sigmaplot 5.0 (Jandel Scientific) as described in ref 6 and references cited therein. SKETCHER permits rapid evaluation of characterizing parameters in the generic set of equations for various kinetic models differing in the number and reactivity of the reactive states by interactive manipulation of calculated curves. Rate equations for reactions in any number of protonic (hydronic) states may be written down without the need for extensive algebraic manipulation by using a simple general model and two information matrices.[26] Those used in the present work are eqs 7–9 which describe reactions in 1, 2, and 3 reactive protonic states severally where K_I–K_{III} are the macroscopic acid dissociation constants and $\tilde{k}_1$–$\tilde{k}_3$ are the pH-independent rate constants.

$$k = \frac{\tilde{k}}{1 + \frac{[H^+]}{K_a}} \quad (7)$$

$$k = \frac{\tilde{k}_1}{1 + \frac{[H^+]}{K_I} + \frac{K_{II}}{[H^+]}} + \frac{\tilde{k}_2}{1 + \frac{[H^+]^2}{K_I K_{II}} + \frac{[H^+]}{K_{II}}} \quad (8)$$

$$k = \frac{\tilde{k}_1}{1 + \frac{[H^+]}{K_I} + \frac{K_{II}}{[H^+]} + \frac{K_I K_{II}}{[H^+]^2}} + \frac{\tilde{k}_2}{1 + \frac{[H^+]^2}{K_I K_{II}} + \frac{[H^+]}{K_{II}} + \frac{K_{III}}{[H^+]}} + \frac{\tilde{k}_3}{1 + \frac{[H^+]^3}{K_I K_{II} K_{III}} + \frac{[H^+]^2}{K_{II} K_{III}} + \frac{[H^+]}{K_{III}}} \quad (9)$$

Computer Modeling of the Quasi-Transition States of the Reactions of Papain with Probes 5–7. This was carried out as described[9] for the reactions of papain with **1**–**4**. The CHARMM force field[27] was used to establish the initial modeled structures as described in ref 28. Probes **5**–**7** were constructed by using the EDITOR module of QUANTA. Structures approximating the transition states of the thiol–disulfide interchange reactions (quasi-transition states) were examined with the catalytic S atoms (Cys25) bonded to the S atom of the probe distal from the mercaptopyridazinyl leaving group. Optimal orientations of the covalently bonded docked ligands were established by performing conformational searches involving rotation of the ligand–Cys25 moiety around defined torsional angles followed by extensive energy minimizations until the change in the potential energy gradient was 0.01 kcal mol^{-1} $Å^{-1}$. The lowest energy conformations of Cys25 and the covalently bonded ligands were then subjected to molecular dynamics simulations. The resulting lowest energy conformations were solvated, and the systems were again energy

minimized until the change in the potential gradient was 0.01 kcal mol^{-1} $Å^{-1}$.

RESULTS

Electronic Absorption Spectra and Ionization Characteristics of 3,3′-Dipyridazinyl Disulfide (5), Its Phenyl (6) and *n*-Propyl (7) Derivatives, and the Common Thiolysis Product Pyridazine-3-thione (12). The spectrum of **5** at pH −0.34 consists of a band with λ_{max} 250 nm and ε_{max} = 1.20 × 10^4 M^{-1} cm^{-1} and a shoulder around 315 nm with ε_{max} = 1.53 × 10^3 M^{-1} cm^{-1}. As the pH is increased to 2.21, both of these features are replaced by a shoulder around 285 nm with an isosbestic point at 282 nm (ε_{282} = 3.88 × 10^3 M^{-1} cm^{-1}). The pK_a value of the monoprotonated form of **5** (0.51) was determined from the pH dependence of ε_{315} (Figure 3) as

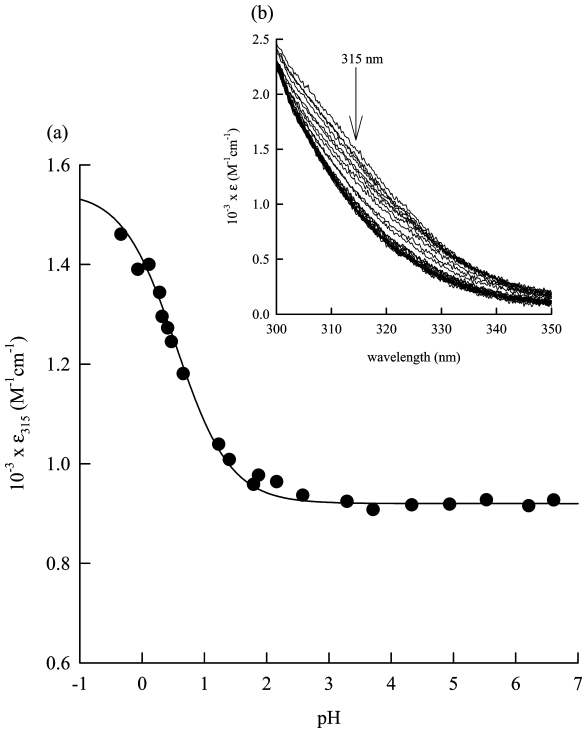

Figure 3. pH dependence of ε_{315} of 3,3′-dipyridazinyl disulfide (**5**). The points in (a) are taken from the scans in (b), and the continuous line in (a) is theoretical for eq 5 of the text with $\tilde{\varepsilon}_1$ = 1.55 × 10^3 M^{-1} cm^{-1}, $\tilde{\varepsilon}_2$ = 9.20 × 10^2 M^{-1} cm^{-1}, and pK_a 0.51.

described in the Experimental Procedures. The pK_a values of the monoprotonated forms of **6** and **7**, similarly determined, are 0.92 and 1.23, respectively. The pK_a values of the monoprotonated forms of the 3-pyridazinyl probes **5**−**7** are comparable to the pK_a value (0.91) of the monoprotonated form of 4,4′-dipyrimidyl disulfide.[29] The only pK_a value (8.26) observed for **12** in the pH region 1.22−11.89 (Figure 4) is characteristic of proton loss from the neutral thione for which Albert and Barlin[30] reported a pK_a value of 8.30. The pK_a value of the monocation of **12** was reported to be −2.68.[30]

Hydrogen-Bonding Interactions Involving Papain and the Reactivity Probes 5−8 Revealed by Computer Modeling of Quasi-Reaction Transition States. The modeled structures of the quasi-transition states of the reactions of papain with the three pyridazinyl probes **5**−**7** and 4,4′-dipyrimidyl disulfide (**8**) are shown in Figures 5−8. In

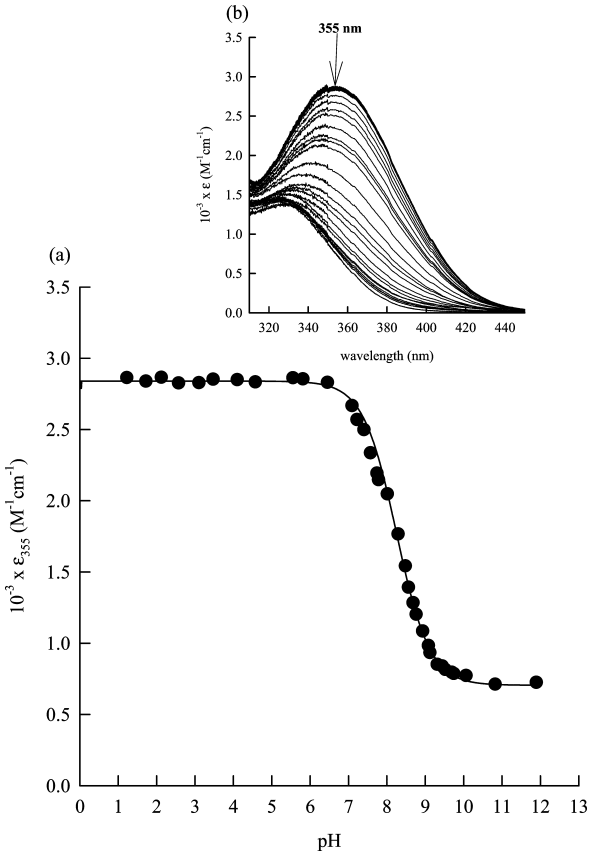

Figure 4. pH dependence of ε_{355} of pyridazine-3-thione (**12**), the thiolysis product of **5**. The points in (a) are taken from the scans in (b), and the continuous line in (a) is theoretical for eq 5 of the text with $\tilde{\varepsilon}_1$ = 2.83 × 10^3 M^{-1} cm^{-1}, $\tilde{\varepsilon}_2$ = 7.05 × 10^2 M^{-1} cm^{-1}, and pK_a 8.26.

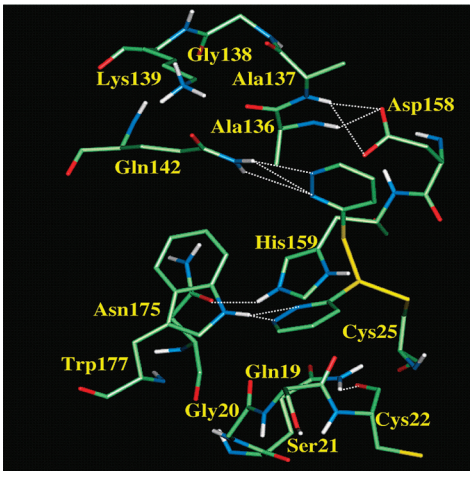

Figure 5. Model of the quasi-transition state of the reaction of papain with of 3,3′-dipyridazinyl disulfide (**5**). Both N-3 and N-4 atoms of the 3-mercaptopyridazine leaving group engage in fluctuant hydrogen-bonding interactions with the amide side chain −NH_2 of Gln142. Both N-2 and N-3 atoms of the nonleaving group engage in fluctuant hydrogen-bonding interactions with the indole side chain −NH of Trp177 which interrupts the hydrogen-bonding interaction of the carbonyl O atom of the amide side chain of Gln19 and the indole side chain N−H of and Trp177.

the interactions with the symmetrical pyridazinyl probe **5** (Figure 5), both N-2 and N-3 of the 3-mercaptopyridazine

dx.doi.org/10.1021/bi201207z | *Biochemistry* 2011, 50, 10732−10742

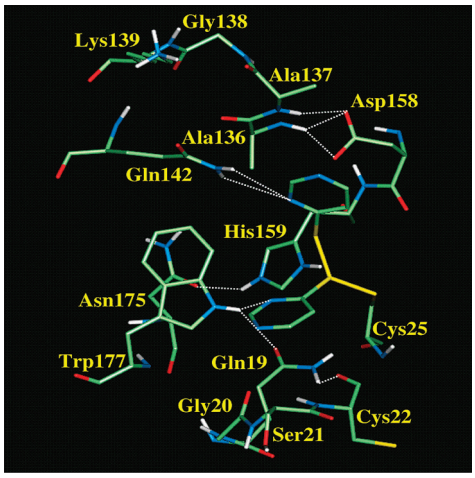

Figure 6. Model of the quasi-transition state of the reaction of papain with of 4,4′-dipyrimidyl disulfide (**8**). The N-2 atom of the 4-mercaptopyrimidine leaving group engages in hydrogen-bonding interactions with the amide side chain $-NH_2$ of Gln142. The N-2 atom of the nonleaving group engages in hydrogen-bonding interactions with the indole side chain N−H of Trp177 which also hydrogen bonds with the carbonyl O atom of the amide side chain of Gln19.

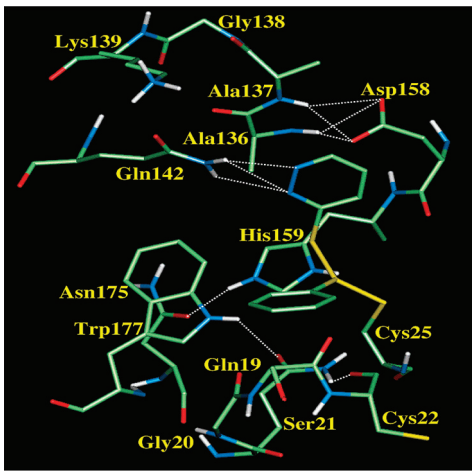

Figure 7. Model of the quasi-transition state of the reaction of papain with of phenyl 3-pyridazinyl disulfide (**6**). Both N-2 and N-3 atoms of the 3-mercaptopyridazine leaving group engage in hydrogen-bonding interactions with the amide side chain $-NH_2$ of Gln142. The nonleaving group is devoid of hydrogen-bonding sites, and the hydrogen bond between the indole side chain N−H of Trp177 and the carbonyl O of the amide side chain of Gln19 is not interrupted.

leaving group engage in hydrogen-bonding interactions with the amide side chain $-NH_2$ group of Gln142. Both N atoms of the nonleaving group engage in fluctuant hydrogen-bonding interactions with the indole side chain N−H of Trp177. As in the interactions with **5**, N-2 of the leaving group of the symmetrical pyrimidyl probe **8** accepts hydrogen bonds from the amide side chain of Gln142, but in contrast to the hydrogen-bonding interactions with N-3 of **5**, there are no such interactions with N-4 of **8** (Figure 6). Only N-2 (i.e., not also N-4) of the nonleaving group of **8** engages in fluctuant interaction with the indole side chain N−H of Trp177. It is noteworthy that (a) the Trp177 N−H also donates a fluctuant hydrogen bond to the carbonyl O of the amide side chain of Gln19 and (b) this hydrogen bond, which exists in unliganded

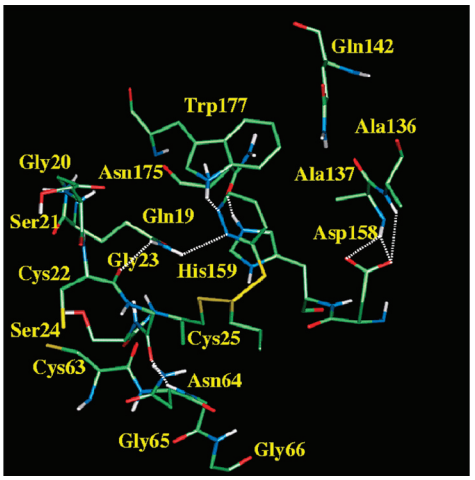

Figure 8. Model of the quasi-transition state of the reaction of papain with of *n*-propyl-3-pyridazinyl disulfide (**7**). The binding mode of this disulfide inhibitor is markedly different from those of the other inhibitors **5**, **6**, and **8** shown in Figures 5−7: thus, N-2 and N-3 atoms of the leaving group of **7** accept hydrogen bonds from the side chains of Gln19 and Trp177, respectively, which interrupt the direct hydrogen-bonding interaction between these side chains shown in Figure 7.

papain, does not exist in the quasi-transition state model of the reaction of papain with **5** (Figure 5).

In the model of the quasi-transition state of the reaction of papain with phenyl-3-pyridazinyl disulfide, **6** (Figure 7), the amide side chain $-NH_2$ group of Gln142 donates hydrogen bonds to N-2 and N-3 of the leaving group as with the symmetrical pyridazinyl probe **5**. Hydrogen-bonding opportunities with the phenyl ring of the nonleaving group of **6** do not exist, however, and hydrogen bonding of the indole side chain N−H of Trp177 with the carbonyl O of the amide side chain of Gln19 persists. This contrasts with the situation with **5** where this hydrogen bond is absent.

The modeled structure of the quasi-transition state of the reaction of papain with *n*-propyl-3-pyridanzinyl disulfide, **7** (Figure 8), shows the binding mode to be entirely different from those in Figures 5−7. The N-2 atom of the pyridazinyl ring of the leaving group accepts a hydrogen bond from the amide side chain $-NH_2$ group of Gln19 rather than from Gln142, as it does with **5** and **6**, and N-3 accepts a hydrogen bond from the amide side chain N−H of Trp177. This unique binding mode prevents direct interaction between Gln19 and Trp177.

Kinetic Characteristics of the Reactions of Papain with the Pyridazinyl Reactivity Probes 5−7 and 4,4′-Dipyrimidyl Disulfide (8). The kinetic and modeling studies of the reactions of papain with **5**−**7** and the modeling studies of the reaction with **8**, here reported, have as their basis the kinetic studies of the reaction of papain with **8**[6,29] minimally refined in the present work.

Reaction of Papain with 8. The pH dependence of the second-order rate constant (k) of this reaction is shown in Figure 9A. The major features of the pH−k profile are a reactive protonic state ($\tilde{k}$ = 2.05 × 10^3 M^{-1} s^{-1}) produced as the pH is increased across one free enzyme pK_a of 3.35 and another ($\tilde{k}$ = 4.20 × 10^4 M^{-1} s^{-1}) produced across a free enzyme pK_a of 8.34. The former corresponds to formation of the intimate (Cys25)-S^-/(His159)-Im^+H ion pair of the catalytic site and the latter to the formation of the

dx.doi.org/10.1021/bi201207z | *Biochemistry* 2011, 50, 10732−10742

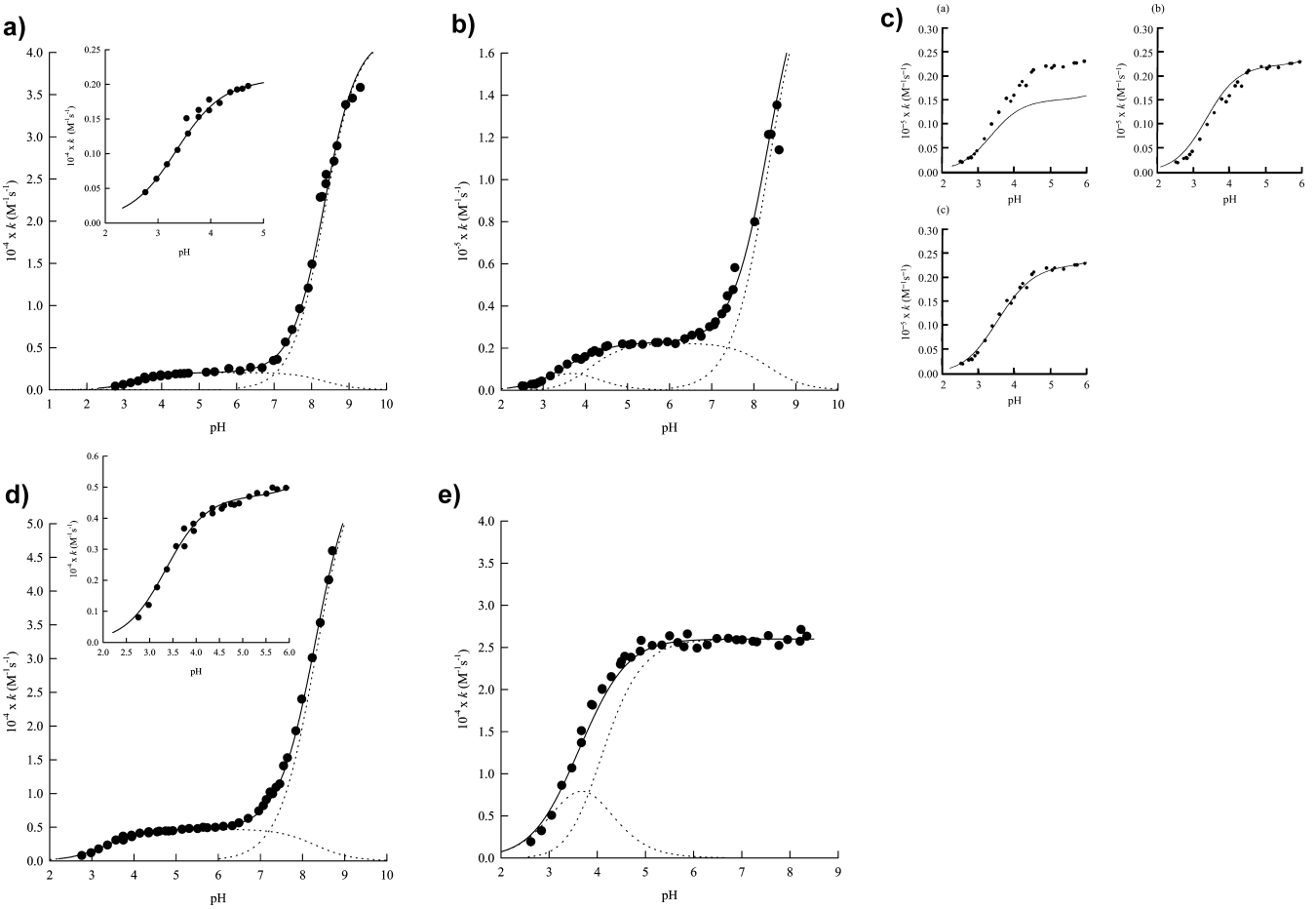

Figure 9. pH dependences of the second-order rate constants (k) for the reactions at 25 °C and I = 0.1 M of papain with (A) of 4,4′-dipyrimidyl disulfide (**8**), (B, C) 3,3′-dipyridazinyl disulfide (**5**), (D) phenyl 3-pyridazinyl disulfide (**6**), and (E) *n*-propyl-3-pyridazinyl disulfide (**7**). In all cases, the data points are mean values of at least three determinations of k at a given pH with standard deviation values of <±10% of the means (see Experimental Procedures). The solid lines are theoretical for eqs 3−5 of the text, and the values of the characterizing parameters, macroscopic pK_a values, and pH-independent rate constants $\tilde{k}_1$−$\tilde{k}_3$ in M^{-1} s^{-1} are given below. The broken lines correspond to contributions to k of the individual protonic states of the reactions provided by the individual terms of the right-hand sides of eqs 3−5. The values of the characterizing parameters are for (A) pK_I = 0.91, pK_{II} = 3.35, pK_{III} = 8.34, $\tilde{k}_1$ = 50, $\tilde{k}_2$ = 2.05 × 10^3, and $\tilde{k}_3$ = 4.20 × 10^4; the inset in (A) which shows the data in the pH range 2.8−4.8 and the solid line theoretical for eq 3 with pK_a = 3.35 and $\tilde{k}$ = 2.05 × 10^3 demonstrate the absence of an additional pK_a value of 4.0; for (B) pK_I = 3.26, pK_{II} = 4.09, pK_{III} = 8.34, $\tilde{k}_1$ = 1.40 × 10^4, $\tilde{k}_2$ = 2.25 × 10^4, and $\tilde{k}_3$ = 2.10 × 10^5; pK_I is the macroscopic pK_a resulting from the proximity of pK_a 3.35 (the pK_a for ion pair formation) to pK_a 4.0 (the electrostatic modulator pK_a which is shifted to the macroscopic pK_a of 4.09; these shifts apply also in (C, c) and in (E) below; for (C, a) pK_I = 3.35, pK_{II} = 8.34, $\tilde{k}_1$ = 1.50 × 10^4, and $\tilde{k}_2$ = 2.10 × 10^5; for (C, b) pK_I = 3.35, pK_{II} = 8.34, $\tilde{k}_1$ = 2.23 × 10^4, and $\tilde{k}_2$ = 2.10 × 10^5; for (C, c) pK_I = 3.26, pK_{II} = 4.09, pK_{III} = 8.34, $\tilde{k}_1$ = 1.40 × 10^4, $\tilde{k}_2$ = 2.25 × 10^4, and $\tilde{k}_3$ = 2.10 × 10^5; for (D) pK_I = 3.35, pK_{II} = 8.34, $\tilde{k}_1$ = 4.72 × 10^3, and $\tilde{k}_2$ = 6.0 × 10^4; the inset in (D) which shows the data in the pH range 2.8−6.0 demonstrates a good fit of the data to pK_a 3.35 (the pK_a for ion pair formation) and the absence of an additional pK_a of 4.0; for (E) pK_I = 3.26, pK_{II} = 4.09, $\tilde{k}_1$ = 1.40 × 10^4, and $\tilde{k}_2$ = 2.60 × 10^4. The lack of a good fit of the data in (C, a) and (C, b) and the good fit in (C, c) demonstrate the kinetic influence of the electrostatic modulator with pK_a 4.0. The absence of a kinetically influential pK_a of 8.34 characteristic of the deprotonation of the ion pair to produce the noncatalytic the (Cys25)-S^-/(His159)-Im anion is noteworthy (see the Discussion).

uncomplicated (noncatalytically active) thiolate anion (Cys25)-S^-/(His159)-Im. These pK_a values of kinetically influential deprotonations are detected by a number of other reactivity probes summarized in ref 13. Inclusion of the expected pK_a of 0.91 characteristic of deprotonation of the probe monocation[29] leading to the formation of a minor reactive state of low observed reactivity ($\tilde{k}$ = 50 M^{-1} s^{-1}) provides a small improvement of the fit to the data in Figure 9A. This minor state corresponds to reaction of the low concentration of enzyme ion pair at low pH with the monocationic form of the probe. It is noteworthy that the inset in Figure 9A provides no evidence for the additional pK_a of 4.0 that is attributed to the electrostatic modulator of catalytic activity detected in catalysis[6,13] and also in the reaction of papain with 3,3′-dipyridazinyl disulfide (**5**) (see below).

Reaction of Papain with 5: Provision of Additional Hydrogen-Bonding Opportunities in Both Leaving Group and Nonleaving Group Parts of the Probe. The pH−k profile for this reaction shown in Figure 9B,C requires three free enzyme pK_a values: those known to be related to the formation (3.35) and deprotonation (8.34) of the (Cys25)-S^-/(His159)-Im^+H ion pair state and that (4.0) of the postulated electrostatic modulator.[13] The microscopic (group) pK_a value 3.35 is that observed in reactions of some reactivity probes such as **8** in which pK_a 4 is not observed, and pK_a 4 is that observed in catalysis in the absence of pK_a 3.35.[13] In cases such as the reaction with **5**, where both pK_a values are kinetically

significant, the pH−k profiles are characterized by macroscopic (molecular) pK_a values.

The phenomenon of overlapping ionizations[31] and the relationships between various types of acid dissociation constant have been widely discussed in relation to the ionisations of a two-site acid e.g. in ref 32. The shift in pK_a values from group to molecular, calculated when the former are known from independent experiments, is symmetrical as illustrated in Figure 9C, where the observed molecular pK_a values (3.26 and 4.09) are shifted from the known group pK_a values by ±0.09. The necessity to include the pK_a of the modulator to obtain a good fit of the data in acidic media is compelled by its omission in Figure 9C,a,b and its inclusion in Figure 9C,c.

Kinetic Consequences of the Omission of the Hydrogen-Bonding Opportunities in the Nonleaving Ring of the Probe: Reaction with the Phenyl Pyridazinyl Disulfide 6. The pH−k profile for the reaction of papain with **6** (shown in Figure 9D) is of double sigmoidal from with pK_a values 3.35 and 8.34. These are characteristic of the formation of the (Cys25)-S^-/(His159)-Im^+H ion pair state and its deprotonation to form (Cys25)-S^-/(His159)-Im, respectively. The absence in Figure 9D of the kinetic influences of the ionization with pK_a 4 seen in Figure 9C for the reaction of the symmetrical pyridazinyl disulfide **5** in which opportunities for hydrogen-bonding interactions exist in both parts of the probe molecule is demonstrated in the inset of Figure 9D, showing an expansion of the data in acidic media.

Kinetic Consequences of Replacing the Rigid Phenyl Ring in 6 by the Smaller Flexible *n*-Propyl Group in 7. The pH−k profile for the reaction of papain with the *n*-propyl pyridazinyl probe **7** (shown in Figure 9E) is characterized by pK_a values for the formation of the (Cys25)-S^-/(His159)-Im^+H ion pair state (3.35) and the electrostatic modulator (4.0) observed in the mixed values (3.26 and 4.09, respectively). The observation of the influence of pK_a 4.0 contrasts with its absence in the reactions with the phenyl probe **6** (Figure 9D). This and the unexpected lack of the increase in reactivity across pK_a 8.3 consequent on deprotonation of the Cys/His ion pair state are considered further in the Discussion section whether the kinetic data for the reactions of the four probes **5**−**8** are interpreted using the modeled structures of the quasi-transition states.

DISCUSSION

As discussed in the Introduction, the results from a combination of reactivity probe kinetics using 2-pyridyl and 4-pyrimidyl disulfides, pH-dependent kinetics of catalysis, electrostatic potential calculations, and normal-mode analysis[6,7,9] revealed that the historic role of the catalytic site Cys/His pair of the cysteine proteinases needs to be understood within the context of additional dynamic phenomena. The objective of the work reported in the present paper was to identify nonelectrostatic interactions involved in the development of both nucleophilic reactivity in the Cys/His ion pair and catalytic competence in papain, in many respects the cysteine proteinase archetype.

The evidence reported previously from the use of the cationic probes **1**−**4**[9] suggested that the focus in the present paper should be on variation in the hydrogen-bonding interactions with the indole side chain N−H of Trp177 and the potential consequences for ion pair geometry and the key kinetic influence in catalysis[6] of the remote ionization with pK_a 4. Initially, the modeled structures of the quasi-transition states of the reactions of papain with the symmetrical probes 3,3′-dipyridazinyl disulfide **5** (Figure 5) and 4,4′-dipyrimidyl disulfide **8** (Figure 6) were compared. The potential hydrogen-bonding acceptor atoms N-2 of both the leaving group and the nonleaving group are common to both **5** and **8**, but the locations of the other acceptor atoms differ, being N-3 in the pyridazinyl probe and N-4 in the pyrimidyl probe. In Figure 6 the hydrogen bonding between the indole side chain N−H of Trp177 and the carbonyl O of the amide side chain of Gln19, a constituent of the oxyanion hole of native papain,[12] is maintained even though a transient hydrogen bond exists also between Trp177 N−H and N-2 of the nonleaving group of **8**. The binding mode also involves hydrogen bonding between the amide side chain $-NH_2$ group of Gln142 and N-2 of the leaving group. The modeled structure in Figure 6 contrasts in what appears to be of potential mechanistic significance with that of the quasi-transition state of the reaction of papain with 3,3′-dipyridazinyl disulfide **5** (Figure 5). Thus, Trp177 is hydrogen bonded more firmly with the nonleaving group of **5** by interactions with both N-2 and N-3, and the hydrogen bond between Trp177 and Gln19 is disrupted. Likewise, Gln142 is hydrogen bonded to both N-2 and N-3 of the leaving group of **5** which contributes to the geometry of the binding mode.

The differences revealed in the two quasi-transition state models (Figures 5 and 6) correlate with mechanistically relevant differences in the pH-dependent kinetic characteristics demonstrated in Figure 9A−C. Thus, in the reaction of papain with the symmetrical pyrimidyl probe **8** via the quasi-transition state in which the Trp177−Gln19 hydrogen bond is maintained (Figure 6), there is no evidence in the pH−k profile (Figure 9A) for a kinetically influential pK_a of 4. By contrast, in the reaction with the symmetrical pyridazinyl probe **5** via the quasi-transition state in which the interaction between the indole side chain N−H of Trp177 and the carbonyl O of the amide side chain of Gln19 is disrupted as a consequence of the hydrogen bonds between Trp177 and N-2 and N-3 of the nonleaving group of **5** (Figure 5), the kinetic influence of a pK_a of 4 is clearly apparent (Figure 9B,C). Geometric changes in a key region of the catalytic site of papain containing both Trp177, the hydrophobic shield of the (Cys25)-S^-/(His159)-Im^+H ion pair, and a component (Gln19) of the oxyanion hole whose role is stabilization of the transient tetrahedral species in the acylation step of the catalytic act are noteworthy. This is particularly so because it appears to correlate with the transmission of the effect of the postulated electrostatic modulator to the catalytic site and with the movement of Trp177 with consequent release of nucleophilic reactivity in Cys25 by decrease in its solvation by His159.[9] The existence of the oxyanion hole was suggested by the crystallographic study of (Z)-L-Phe-L-Ala methylene papain reported by Drenth et al.[33] This feature could stabilize the developing oxyanion bonded to the developing tetrahedral carbon atom of the substrate by a hydrogen-bonded network involving the −NH peptide backbone of the peptide backbone of Cys25 and the amide side chain $-NH_2$ group of Gln19. Evidence for the functional role of the oxyanion hole is provided by the extensive protein engineering studies reported by Storer and colleagues[34,35] reviewed in ref 12. One interpretation suggested to explain the decreases in k_{cat} for the Gln19Ser and Gln19Ala mutants was the changes in the degree of solvation of the oxyanion as a result of the shortening of the Gln19 side chain and the consequent cavity formation.

To further test the conclusion suggested by the pH−k profiles for the reactions of **5** and **8**, the investigation of the pH dependences of the reactions of papain with two other new probes **6** and **7** in which the nonleaving group is unable to engage in hydrogen bonding was undertaken. Phenyl-3-pyridazinyl disulfide (**6**) and *n*-propyl-3-pyridazinyl disulfide (**7**) were readily synthesized from the new symmetrical probe 3,3′-dipyridazinyl disulfide (**5**). The symmetrical probe was obtained by the six-step synthesis (Figure 2) described in Experimental Procedures, and its reaction with thiophenyl or *n*-propanethiol readily provided **6** or **7**, respectively.

The phenyl 3-pyridazinyl disulfide probe **6** is similar in steric occupancy to **5** but without the hydrogen-bonding opportunities in the ring of the nonleaving group. As in the model of the quasi-transition state of the reaction of papain with **5** (Figure 5), N-2 and N-3 of the leaving group of **6** are hydrogen bonded to the amide side chain $-NH_2$ group of Gln142 (Figure 7). A noteworthy difference between Figures 5 and 7 is that the Trp177−Gln19 hydrogen bond, which is disrupted in Figure 5 is maintained in Figure 7. It is noteworthy also that the kinetically influential pK_a 4 clearly demonstrated in Figure 9C for the reaction of **5** is absent in Figure 9D for the reaction of **6**. These results from the combination of quasi-transition state modeling and pH-dependent kinetics for the reactions of **5** and **6** emphasize the connection between the disruption of the Trp177−Gln19 hydrogen bond and the manifestation of the kinetic influence of the pK_a of 4 essential for the development of catalytic activity suggested to be associated with the electrostatic modulator.

Presumably the steric occupancy of the phenyl ring of the nonleaving group in the region around Trp177 and His159 even without the hydrogen-bonding interactions with Trp77 together with the hydrogen-bonding interactions of the pyridazinyl ring of the leaving group with Gln12 common to **5** and **6** in sufficient to maintain a generally similar quasi-transition state binding mode in Figures 5 and 7. In marked contrast to this binding mode, that of the quasi-transition state for the reaction of papain with the less rigid *n*-propyl-3-pyridazinyl disulfide (**7**) (Figure 8) differs in two interesting respects from those in Figures 5 and 7. First, the general binding mode places the pyridazinyl ring of the leaving group in the vicinity of Trp177 and Gln19 rather than in the vicinity of Gln142, and second there is no direct hydrogen-bonding interaction between Trp177 and Gln19. Rather hydrogen bonds are donated to N-2 and N-3 of the leaving group by Gln19 and Trp177, respectively. The lack of a direct Trp177−Gln19 hydrogen bond correlates with the presence of a kinetically influential pK_a of 4 in the pH−k profile for the reaction of *n*-propyl-3-pyridazinyl disulfide (**7**) (Figure 9E). This is consistent with the presence of pK_a 4 for the reaction of the symmetrical probe 3,3′-dipyridazinyl disulfide (**5**) (Figure 9C) and the lack of a Trp177−Gln19 hydrogen bond in the quasi-transition state of this reaction (Figure 5). An unexpected feature of the pH−k profile (Figure 9E) for the reaction of the *n*-propyl-3-pyridazinyl disulfide (**7**) is the absence of any increase in reactivity in the pH range 7−8 from the values of $\tilde{k}_2$ = 2.60 × 10^4 M^{-1} s^{-1} following formation of the Cys/His ion pair and its modulation across pK_a 4.09. Increase in k above pH 7 is a common feature of many reactions of the thiol group of papain,[12] including those in Figure 9A,B,D, resulting from the higher reactivity of the anion (Cys25)-S^-/(His159)-Im than that of the ion pair (Cys25)-S^-/(His159)-Im^+H. The reactivities of the ion pair of papain before and after modulation by pK_a 4 in the reactions with **5** and **7** are similar (for **5** $\tilde{k}_1$ = 1.40 × 10^4 M^{-1} s^{-1}, $\tilde{k}_2$ = 2.25 × 10^4 M^{-1} s^{-1}, and $\tilde{k}_3$ = 2.10 × 10^5 M^{-1} s^{-1}; for **7** $\tilde{k}_1$ = 1.40 × 10^4 M^{-1} s^{-1} and $\tilde{k}_2$ = 2.60 × 10^4 M^{-1} s^{-1}; see Figure 9B,E). This suggests that the absence of further increase in k above pH 7 in the reaction of **7** which contrasts with the increase in k for the reactions of **5** from to $\tilde{k}_2$ = 2.25 × 10^4 M^{-1} s^{-1} to $\tilde{k}_3$ = 2.10 × 10^5 M^{-1} s^{-1} across pK_a 8.34 is due to the maintenance of the ion pair state beyond pH 8 in this reaction. In the binding mode of **7** the difference in the relative positions of the pyridazinyl and imidazolium rings from those in the reaction with **5** suggests that the ion pair of papain in its reaction with **7** might be relatively stabilized due to inhibition of physical movement of (His 159)-Im^+H and/or to increase in its pK_a by the proximity of N-2 of the pyridazinyl ring. This phenomenon may be compared with the stabilization of the (Cys25)-S^-/(His159)-Im^+H ion pair of papain in its reaction with the cationic 2-pyridyl probe **1** but not in that with the analogous but longer probe **4** detected by the marked difference between the two pH−k profiles in acidic media.[9] In the reaction with **1** the mutual solvation of the ion pair components is maintained because the movement of Trp 177 is contained within the symmetrically moving walls of the cleft. By contrast in the reaction with **4** the motion of the cleft is antisymmetric around the Trp 177 region which results in His 159 being exposed to solvent.[9]

A significant advance in understanding the mechanism of catalysis by members of the papain family resulted from the demonstration that the development of catalytic activity across pK_a 4 is not due to the formation of the intimate (Cys25)-S^-/(His159)-Im^+H ion pair of the catalytic site, which was shown to occur across lower pK_a values. Rather, it was suggested that pK_a 4 be assigned to Glu35, a component of the Glu50 cluster, on the basis of its interaction energy with the catalytic site ion pair.[6] The present work provides further insight into the mechanism by establishing that the kinetic influence of pK_a 4 correlates with the interruption of the Trp177−Gln19 hydrogen bond. This is predicted to facilitate the movement of Trp177 detected by normal-mode analysis[9] which results in His159 (papain numbering) being exposed to solvent with consequent decrease in its solvation of the thiolate anion of Cys25. Evidence for a strong interaction between the thiolate anion and the imidazolium cation of the intimate ion pair in native papain is the exceedingly low pK_a of the thiol group, 3.35,[6] relative to the pK_a of an isolated thiol group in an aqueous environment (~8.5). The unusually low pK_a is considered to be a consequence of the mutual solvation of the ion pair components permitted by the water-free hydrophobic microenvironment provided by the indole ring of Trp177.[36] The anionic−cationic interaction is predicted to result in low nucleophilic reactivity of the ion pair S atom as in the case for an un-ionized thiol group. It has long been appreciated that the Cys25 and His159 components, being on opposite sides of the active center cleft,[36] are susceptible to movement. When the movement of the cleft is antisymmetric around the Trp177 region, His159 moves to become solvated by water.[9] This decreases its strong influence on the thiolate anion of Cys-25 with an expectation of consequent development of nucleophilic reactivity characteristic of a thiolate anion freed from its cationic partner. This is required for cleavage of the scissile bond of the substrate leading to the transient rate-determining formation of the thiolester intermediate during catalysis. An additional consequence of the disruption of the Trp177−Gln19 interaction might be an increase in the

effectiveness of the oxyanion hole in binding the developing tetrahedral species during the acylation process.

AUTHOR INFORMATION

Corresponding Author

*Tel: 00 44 207 882 6332. Fax: 00 44 208 0973. E-mail: kb1@qmul.ac.uk.

Present Address

[⊥]European ScreeningPort GmbH, Schnackenburgallee 114, 22525 Hamburg, Germany.

Funding

We acknowledge research studentships from the Engineering and Physical Sciences Research Council for A.K. and S.G. and from the Biotechnology and Biological Sciences Research Council for S.H.

ABBREVIATIONS

Im^+H, imidazolium; Im, imidazole; 2-Py, 2-pyridyl.

REFERENCES

(1) Brocklehurst, K., Gul, S., and Pickersgill, R. W. (2009) Substrate Recognition, in *Amino Acids, Peptides and Proteins in Organic Chemistry* (Hughes, A. B., Ed.) Vol. *2*, pp 475−506, Wiley-VCH Publishers, New York.

(2) Kowlessur, D., Topham, C. M., Thomas, E. W., O'Driscoll, M., Templeton, W., and Brocklehurst, K. (1989) Identification of signalling and non-signalling binding contributions to enzyme reactivity. Alternative combinations of binding interactions provide for change in transition-state geometry in reactions of papain. *Biochem. J. 258*, 755−764.

(3) Kowlessur, D., O'Driscoll, M., Topham, C. M., Templeton, W., Thomas, E. W., and Brocklehurst, K. (1989) The interplay of electrostatic fields and binding interactions determining catalytic-site reactivity in actinidin. A possible origin of differences in the behaviour of actinidin and papain. *Biochem. J. 259*, 443−452.

(4) Patel, M., Kayani, S., Templeton, W., Mellor, G. W., Thomas, E. W., and Brocklehurst, K. (1992) Evaluation of hydrogen bonding and enantiomeric P_2-S_2 hydrophobic contacts in dynamic aspects of molecular recognition by papain. *Biochem. J. 287*, 881−889.

(5) Taylor, M. A. J., Baker, K. C., Connerton, I. F., Cummings, N. J., Harris, G. W., Henderson, I. M., Jones, S. T., Pickersgill, R. W., Sumner, I. G., Warwicker, J., and Goodenough, P. W. (1994) An unequivocal example of cysteine proteinase activity affected by multiple electrostatic interactions. *Protein Eng. 10*, 1267−1276.

(6) Pinitglang, S., Watts, A. B., Patel, M., Reid, J. D., Noble, M. A., Gul, S., Bokth, A., Naeem, A., Patel, H., Thomas, E. W., Sreedharan, S. K., Verma, C., and Brocklehurst, K. (1997) A classical enzyme active center motif lacks catalytic competence until modulated electrostatically. *Biochemistry 36*, 9968−9982.

(7) Gul, S., Mellor, G. W., Thomas, E., and Brocklehurst, K. (2006) Temperature-dependences of the kinetics of reactions of papain and actinidin with a series of reactivity probes differing in key molecular recognition features. *Biochem. J. 396*, 17−21.

(8) O'Farrell, P. A., and Joshua-Tor, L. (2007) Mutagenesis and crystallographic studies of the catalytic residues of the papain family protease bleomycin hydrolase: New insights into active-site structure. *Biochem. J. 401*, 421−428.

(9) Gul, S., Hussain, S., Thomas, M. P., Resmini, M., Verma, C. S., Thomas, E. W., and Brocklehurst, K. (2008) Generation of nucleophilic character in the Cys25/His159 ion pair of papain involves Trp177 but not Asp158. *Biochemistry 47*, 2025−2035.

(10) Barrett, A. J., Rawlings, N. D., and Woessner, Jr., J. F., Eds. (2004) *Handbook of Proteolytic Enzymes*, Elsevier, London.

(11) Brocklehurst, K., Willenbrock, F., and Salih, E. (1987) Cysteine proteinases, in *Hydrolytic Enzymes: New Comprehensive Biochemistry* (Neuberger, A., and Brocklehurst, K., Eds.) Vol. *16*, pp 39−158, Elsevier, Amsterdam.

(12) Brocklehurst, K., Watts, A. B., Patel, M., Verma, C. S., and Thomas, E. W. (1998) Cysteine proteinases, in *Comprehensive Biological Catalysis* (Sinnot, M. L., Ed.) Vol. *1*, pp 381−423, Academic Press, London.

(13) Hussain, S., Khan, A., and Brocklehurst, K. (2002) A review of developments in the study of cysteine proteinase mechanism: Opportunities for the investigation of electrostatic effects and dynamic aspects of molecular recognition in enzyme chemistry. *Recent Res. Dev. Biochem. 3*, 653−677.

(14) Topham, C. M., Salih, E., Frazao, C., Kowlessur, D., Overington, J. P., Thomas, M., Brocklehurst, S. M., Patel, M., Thomas, E. W., and Brocklehurst, K. (1991) Structure-function relationships in the cysteine proteinases actinidin, papain and papaya proteinase Ω. *Biochem. J. 280*, 79−92.

(15) Noble, M. A., Gul, S., Verma, C. S., and Brocklehurst, K. (2000) Ionization characteristics and chemical influences of aspartic acid residue 158 of papain and caricain determined by structure-related kinetic and computational techniques: multiple electrostatic modulators of active-centre chemistry. *Biochem. J. 351*, 723−733.

(16) Hussain, S., Pinitglang, S., Bailey, T. S., Reid, J. D., Noble, M. A., Resmini, M., Thomas, E. W., Greaves, R. B., Verma, C. S., and Brocklehurst, K. (2003) Variation in the pH-dependent pre-steady-state and steady-state kinetic characteristics of cysteine-proteinase mechanism: evidence for electrostatic modulation of catalytic site function by the neighbouring carboxylate anion. *Biochem. J. 372*, 735−746.

(17) Ménard, R., Khouri, H. E., Plouffe, C., Dupras, R., Ripoll, D., Vernet, T., Tessier, D. C., Laberte, F., Thomas, D. Y., and Storer, A. C. (1990) A protein engineering study of the role of aspartate 158 in the catalytic mechanism of papain. *Biochemistry 29*, 6706−6713.

(18) Brocklehurst, K. (1982) Two-protonic-state electrophiles as probes of enzyme mechanism. *Methods Enzymol. 87C*, 427−469.

(19) Baines, B. S., and Brocklehurst, K. (1979) A necessary modification to the preparation of papain from any high-quality latex of *Carica papaya* and evidence for the structural integrity of the enzyme produced by traditional methods. *Biochem. J. 177*, 541−548.

(20) Brocklehurst, K., Carlsson, J., Kierstan, M. P., and Crook, E. M. (1973) Covalent chromatography. Preparation of fully active papain from dried papaya latex. *Biochem. J. 133*, 573−584.

(21) Brocklehurst, K., Carlsson, J., Kierstan, M. P., and Crook, E. M. (1974) Covalent chromatography by thiol-disulfide interchange. *Methods Enzymol. 34*, 531−544.

(22) Brocklehurst, K. (2000) Affinity Separation: Covalent Chromatography, in *Encyclopedia of Separation Science*, Vol. *II*, pp 252−259, Academic Press, London.

(23) Stuchbury, T., Shipton, M., Norris, R., Malthouse, J. P., Brocklehurst, K., Herbert, J. A., and Suschitzky, H. (1975) A reporter group delivery system with both absolute and selective specificity for thiol groups and an improved fluorescent probe containing the 7-nitrobenzo-2-oxa-1,3-diazole moiety. *Biochem. J. 151*, 417−432.

(24) Brocklehurst, K., and Little, G. (1973) Reactions of papain and of low-molecular-weight thiols with some aromatic disulphides. 2,2′-Dipyridyl disulphide as a convenient active-site titrant for papain even in the presence of other thiols. *Biochem. J. 133*, 67−80.

(25) Evans, R. C., and Wiselogle, F. Y. (1945) Studies in the pyridazine series. The absorption spectrum of pyridazine. *J. Am. Chem. Soc. 67*, 60−62.

(26) Brocklehurst, S. M., Topham, C. M., and Brocklehurst, K. (1990) A general kinetic equation for multihydronic state reactions and a rapid procedure for parameter evaluation. *Biochem. Soc. Trans. 18*, 598−599.

(27) Brünger, A. T., and Karplus, M. (1988) Polar hydrogen positions in proteins: empirical energy placement and neutron diffraction comparison. *Proteins 4*, 148−156.

(28) Plou, F. J., Kowlessur, D., Malthouse, J. P., Mellor, G. W., Hartshorn, M. J., Pinitglang, S., Patel, H., Topham, C. M., Thomas, E. W., Verma, C., and Brocklehurst, K. (1996) Characterization of the

electrostatic perturbation of a catalytic site (Cys)-S$^-$/(His)-Im$^+$H ion-pair in one type of serine proteinase architecture by kinetic and computational studies on chemically mutated subtilisin variants. *J. Mol. Biol. 257*, 1088−1111.
(29) Mellor, G. W., Thomas, E. W., Topham, C. M., and Brocklehurst, K. (1993) Ionization characteristics of the Cys-25/His-159 interactive system and of the modulatory group of papain: resolution of ambiguity by electronic perturbation of the quasi-2-mercaptopyridine leaving group in a new pyrimidyl disulphide reactivity probe. *Biochem. J. 290*, 289−296.
(30) Albert, A., and Barlin, G. B. (1962) Ionization constants of heterocyclic substances. Part V. Mercapto-derivatives of diazines and benzodiazines. *J. Chem. Soc.*, 3129−3141.
(31) Brocklehurst, K., Willenbrock, S. J. F., and Salih, E. (1983) Effects of conformational selectivity and overlapping kinetically influential ionizations on the characteristics of pH-dependent enzyme kinetics. Implications of free enzyme pK_a variability in reactions of papain for its catalytic mechanism. *Biochem. J. 211*, 701−708.
(32) Brocklehurst, K. (1994) A sound basis for pH-dependent kinetic studies on enzymes. *Protein Eng. 7*, 291−299.
(33) Drenth, J., Kalk, K. H., and Swen, H. M. (1976) Binding of chloromethyl ketone substrate analogues to crystalline papain. *Biochemistry 15*, 3731−3738.
(34) Menard, R., Carriere, J., Laflamme, P., Plouffe, C., Khouri., H. E., Vernet, T., Tessier, D. C., Thomas, D. Y., and Storer, A. C. (1991) Contribution of the glutamine 19 sidechain to transition state stabilization in the oxyanion hole of papain. *Biochemistry 30*, 8924−8928.
(35) Menard, R., Plouffe, C., Laflamme, P., Vernet, T., Tessier, D. C., Thomas, D. Y., and Storer, A. C. (1995) Modification of the electrostatic environment is tolerated in the oxyanion hole of the cysteine protease papain. *Biochemistry 34*, 464−471.
(36) Kamphuis, I. G., Kalk, K. H., Swarte, M. B., and Drenth, J. (1984) Structure of papain refined at 1.65 Å resolution. *J. Mol. Biol. 179*, 233−256.